BIOCHEMISTRY
including biophysical chemistry & molecular biology

Article

pubs.acs.org/biochemistry

Structural and Functional Characterization of the Acidic Region from the RIZ Tumor Suppressor

Yizhi Sun,[†] Jessica M. Stine,[†] Daniel Z. Atwater,[†] Ayesha Sharmin,[†] J. B. Alexander Ross,[†,‡] and Klára Briknarová*[,†,‡]

[†]Department of Chemistry and Biochemistry, University of Montana, Missoula, Montana 59812, United States
[‡]Center for Biomolecular Structure and Dynamics, University of Montana, Missoula, Montana 59812, United States

ABSTRACT: RIZ (retinoblastoma protein-interacting zinc finger protein), also denoted PRDM2, is a transcriptional regulator and tumor suppressor. It was initially identified because of its ability to interact with another well-established tumor suppressor, the retinoblastoma protein (Rb). A short motif, IRCDE, in the acidic region (AR) of RIZ was reported to play an important role in the interaction with the pocket domain of Rb. The IRCDE motif is similar to a consensus Rb-binding sequence LXCXE (where X denotes any amino acid) that is found in several viral Rb-inactivating oncoproteins. To improve our understanding of the molecular basis of binding of Rb to RIZ, we investigated the interaction between purified recombinant AR and the pocket domain of Rb using nuclear magnetic resonance spectroscopy, isothermal titration calorimetry, and fluorescence anisotropy experiments. We show that AR is intrinsically disordered and that it binds the pocket domain with submicromolar affinity. We also demonstrate that the interaction between AR and the pocket domain is mediated primarily by the short stretch of residues containing the IRCDE motif and that the contribution of other parts of AR to the interaction with the pocket domain is minimal. Overall, our data provide clear evidence that RIZ is one of the few cellular proteins that can interact directly with the LXCXE-binding cleft on Rb.

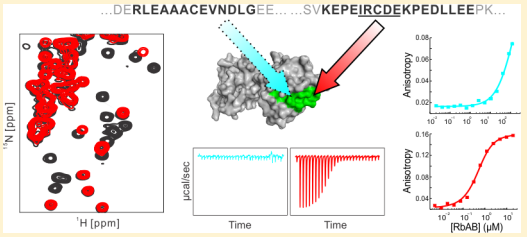

RIZ (retinoblastoma protein-interacting zinc finger protein), also known as PRDM2, is a transcriptional regulator[1−6] from the PRDM protein family.[7,8] The full-length protein (RIZ1) contains a variant of a SET domain called the PR domain, an acidic region (AR), and eight zinc finger motifs that are spread throughout the sequence (Figure 1). Alternative promoter usage results in a shorter product (RIZ2) that starts at M202 and lacks the PR(SET) domain[9] (Figure 1). Gene silencing of RIZ1 but not of RIZ2 is common in many types of human tumors, and inactivation of RIZ1, while preserving RIZ2, causes tumor susceptibility in mouse models.[10−18] Overexpression of RIZ1 in cancer cells results in cell cycle arrest and/or apoptosis.[11,13,17−20]

RIZ binds to the retinoblastoma protein (Rb),[21] a tumor suppressor that regulates the cell cycle, senescence, apoptosis, differentiation, and chromosomal stability.[22−24] A short motif, IRCDE, in the AR of RIZ is required for the interaction.[21] This motif is similar to consensus Rb-binding sequence LXCXE (where X denotes any amino acid) found in several viral Rb-inactivating oncoproteins, including adenoviral E1A protein, E7 protein from papilloma viruses, and large T antigen from simian virus 40 (SV40).[25] The viral LXCXE sequences bind to a shallow groove on cyclin box B of the Rb pocket domain with submicromolar affinity.[26,27] Other regions of the viral proteins (CR1 in E1A, CR3 in E7, and the N-terminal J domain in large T antigen) also interact with Rb and are necessary for Rb inactivation by releasing E2F transcription factors from Rb.[27−29]

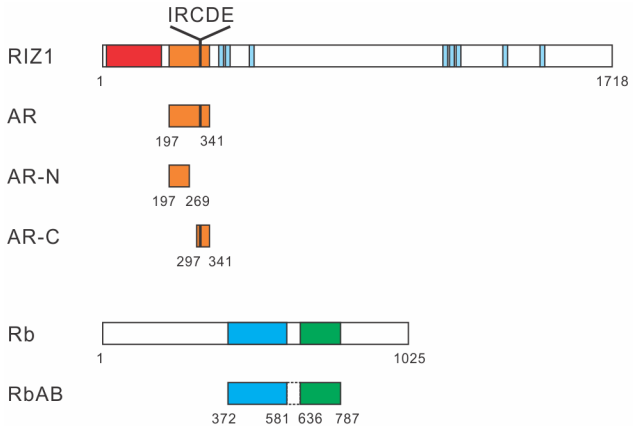

Figure 1. Schematic representation of RIZ1, Rb, and the recombinant constructs used in this study. In RIZ1, the PR(SET) domain is colored red, the acidic region (AR) orange, and the C2H2-like zinc finger domains light blue. The position of the IRCDE motif is indicated. In the Rb protein, cyclin boxes A and B that form the pocket domain are colored blue and green, respectively. The sequence between the cyclin boxes (residues 582−635; dashed) in the RbAB construct is replaced with a two-residue linker (EF).

Received: November 10, 2014
Revised: January 22, 2015
Published: February 2, 2015

DOI: 10.1021/bi501398w
Biochemistry 2015, 54, 1390−1400

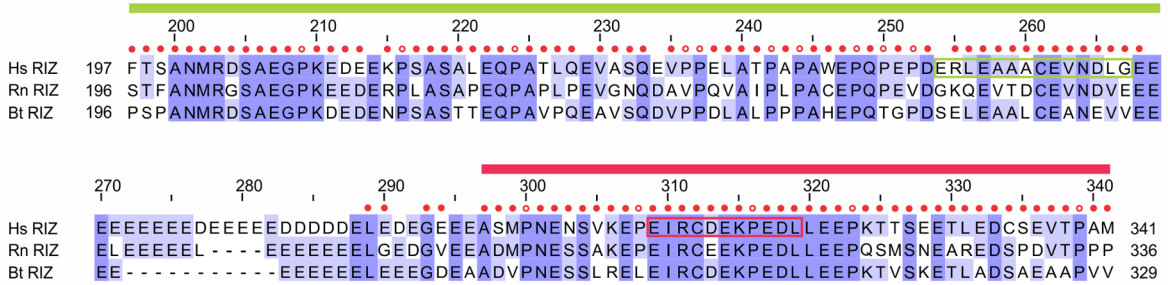

Figure 2. Amino acid sequence of AR. Sequence conservation in RIZ proteins from *Homo sapiens* (Q13029), *Rattus norvegicus* (Q63755), and *Bos taurus* (F1N790) is highlighted by blue shading. The spans of the recombinant AR-N and AR-C protein constructs are shown as green and red bars, respectively, and the peptides used in this study are marked with green and red boxes. The extent of backbone assignment in AR is also indicated. Filled red circles mark residues whose ^{1}H and ^{15}N backbone amide chemical shifts are assigned, and empty red circles denote prolines. AR contains a high proportion of acidic residues, 45 glutamates (30%) and 14 aspartates (9%), and the majority of residues with missing assignments (269−288, 291, 292, 295, and 296) are glutamates and aspartates that are located in the highly degenerate central region of the AR construct. The remaining residues with missing assignments (214, 229, 234, and 254) are glutamates in other parts of AR.

The cleft that interacts with the LXCXE sequences and renders cells susceptible to the pathogenic effects of DNA tumor viruses is one of the most conserved features on Rb, suggesting that it is essential for Rb function.[26] While it is not required for normal development,[30] it was shown to play a role in the establishment of cell senescence in response to γ-irradiation or Ras oncogene,[31] and in suppression of tumorigenesis caused by genotoxins or p53-deficient genetic background.[32−34] Mutations in the LXCXE-binding site on Rb lead to a reduced level of histone H3 K9 trimethylation and a reduced level of repression of E2F-responsive promoters in senescence,[31] a reduced level of histone H4 K20 trimethylation in pericentric heterochromatin,[30] reduced loading of condensin II complexes on chromatin,[33] and centromere fusions, lagging chromosomes, chromosome missegregation, and genomic instability.[30,33] How exactly Rb uses the LXCXE-binding site to regulate all these activities and to suppress tumorigenesis is not well understood. It was reported that the LXCXE-binding site is required for interactions with a number of cellular proteins, including transcriptional factors, histone deacetylases, histone lysine methyltransferases, and other chromatin modification enzymes,[35−40] but whether these interactions are direct or indirect is often unknown or controversial.[35,41,42]

Because RIZ is one of the proteins reported to bind Rb in an LXCXE-dependent manner,[21,43] we investigated the interaction using purified components. We determined that the AR in RIZ is intrinsically disordered, identified the residues within AR that are involved in the interaction with the pocket domain of Rb, and measured the binding affinity. Our results not only unambiguously demonstrate that RIZ and Rb directly interact with submicromolar affinity but also provide further insight into molecular determinants of high-affinity binding between LXCXE-like sequences and Rb.

EXPERIMENTAL PROCEDURES

Proteins and Peptides. Plasmids p3RIZRHQB and pCMV-Rb containing the cDNA sequences of human RIZ1 and Rb, respectively, were provided by S. Huang (State Key Laboratory of Medical Genetics, Central South University, Changsha, Hunan, China). Plasmid pRK793,[44] which was used to express the catalytic domain of tobacco etch virus (TEV) protease, originates from D. Waugh's laboratory and was obtained from Addgene (Addgene plasmid 8827). TEV protease was purified by affinity chromatography on a HisTrap column (GE Healthcare), dialyzed into a buffer containing 50 mM Tris (pH 7.5), 75 mM NaCl, 1 mM ethylenediaminetetraacetic acid (EDTA), 2 mM dithiothreitol (DTT), and 10% glycerol, spiked with additional 2 mM DTT, flash-frozen in liquid nitrogen, and stored at −80 °C until it was used.

The recombinant RIZ constructs and synthetic peptides used in this study are shown in Figures 1 and 2. The DNA sequence encoding the AR of RIZ was amplified from p3RIZRHQB by polymerase chain reaction (PCR) and cloned into the pGEX-4T1 expression vector (GE Healthcare). The AR fused to glutathione transferase (GST) was expressed in *Escherichia coli* BL21-CodonPlus(DE3)-RIL cells (Agilent) and purified by affinity chromatography on glutathione-agarose resin. The GST moiety was subsequently cleaved off with thrombin (Sigma), and the AR was separated from thrombin and GST by affinity chromatography on *p*-aminobenzamidine (pABA) and glutathione-agarose resins, followed by ion-exchange chromatography on a HiTrap Q column (GE Healthcare). The recombinant AR protein contained residues 197−341 of RIZ (FTSA···TPAM) preceded by four extraneous amino acids (GSPE).

The sequences encoding the N- and C-terminal parts of the acidic region (AR-N and AR-C, respectively) were amplified from pGEX-4T1-AR by PCR and cloned into the pDONR 201 vector and subsequently moved into the pDEST 15 vector using the Gateway recombination technology (Life Technologies). TEV cleavage sites at the N-termini of AR-N and AR-C were introduced by primers during the PCR. The AR-N and AR-C fused to GST were expressed in *E. coli* BL21-CodonPlus(DE3)-RIL cells and purified by affinity chromatography on glutathione-agarose resin. The GST moiety was cleaved off with TEV protease, and the AR-N or AR-C was separated from GST and the TEV protease by affinity chromatography on glutathione-agarose resin and by ion-exchange chromatography on a HiTrap Q column. To remove residual GST, some samples were further purified by size-exclusion chromatography on Superdex 75 resin (GE Healthcare). The recombinant AR-N and AR-C proteins contained residues 197−269 (FTSA···LGEE) and 297−341 (ASMP···TPAM) of RIZ, respectively, preceded by three extraneous amino acids (GSG).

The concentrations of the RIZ constructs were calculated from absorbance of the proteins at 280 nm.[45] The concentration of AR-C, which does not contain any tyrosine or tryptophan residues, was determined by a reducing-agent-compatible bicinchoninic acid (BCA) protein assay (Pierce).

DOI: 10.1021/bi501398w
Biochemistry 2015, 54, 1390−1400

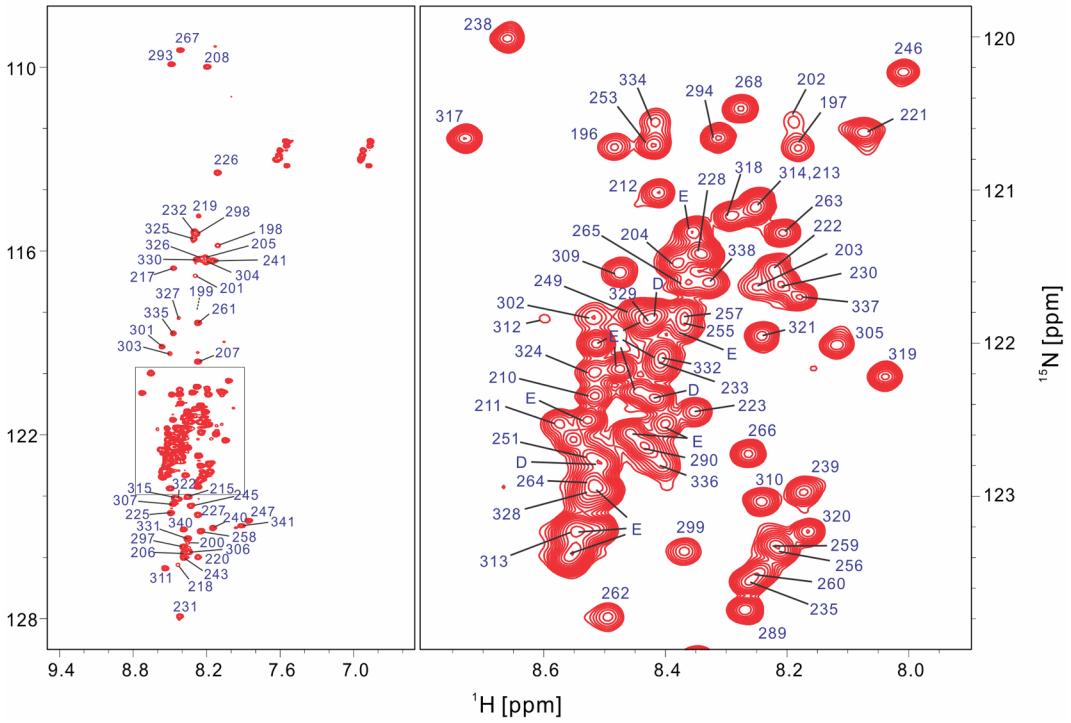

Figure 3. 2D ^{1}H−^{15}N HSQC spectrum of ^{15}N-labeled AR. The crowded central region is shown expanded in the right panel. Sequence specific assignments are indicated, and signals from several aspartates (D) and glutamates (E) that have not been assigned in a sequence specific manner are also labeled.

The assay was calibrated with an AR-C protein containing GWG instead of GSG at the N-terminus.

To prepare the pocket domain of Rb, the DNA sequences encoding cyclin boxes A and B of Rb were amplified separately from pCMV-Rb by PCR and then inserted adjacent to each other into the pGEX-4T1 expression vector; the linker between the cyclin boxes was replaced with an *Eco*RI restriction site in the process. The resulting protein construct (RbAB) fused to GST was expressed in *E. coli* BL21-CodonPlus(DE3)-RIL cells and purified by affinity chromatography on glutathione-agarose resin. The GST moiety was subsequently cleaved off with thrombin, and RbAB was separated from thrombin and GST by affinity chromatography on pABA and glutathione-agarose resins, followed by size-exclusion chromatography on Superdex 75 resin. The recombinant RbAB protein contained two extraneous residues at the N-terminus (GS), residues 372−581 (HTPV···DREG) corresponding to cyclin box A, two connecting residues (EF), and residues 636−787 (FQTQ··· HIPR) corresponding to cyclin box B of Rb (gsHTPV··· DREGefFQTQ···HIPR). The concentration of RbAB was determined from the absorbance at 280 nm.[45]

Fluorescein isothiocyanate (FITC)-labeled peptides corresponding to RIZ(254−267) (ERLEAAACEVNDLG) and RIZ(309−319) (EIRCDEKPEDL), with their C-termini amidated, were obtained from Genscript at >95% purity. The fluorescein was attached to the N-termini of the peptides via a seven-atom aminohexanoyl spacer. The concentrations of stock solutions of the fluorescein-labeled peptides were determined, after dilution into Tris buffer (pH 9.0), from the absorbance at 494 nm using an extinction coefficient of 70000 M^{-1} cm^{-1}.[46] The peptide corresponding to RIZ(309−319), with its N-terminus acetylated and C-terminus amidated, was also obtained from Genscript at >95% purity.

Nuclear Magnetic Resonance (NMR) Spectroscopy. Samples for NMR spectroscopy contained ^{15}N-labeled or ^{13}C- and ^{15}N-labeled RIZ proteins in phosphate-buffered saline (PBS) (pH 7.5) supplemented with 2.5 mM DTT and 10% $^{2}H_2O$. NMR data were acquired at 25 °C on a Varian 600 MHz NMR system that was equipped with a triple-resonance probe or a cold probe. The data were processed with NMRPipe[47] and analyzed with CcpNmr Analysis version 2.2.1.[48]

NMR characterization of AR was accomplished using 0.6 mM ^{15}N-labeled and 0.8 mM ^{13}C- and ^{15}N-labeled protein samples. ^{1}H, ^{13}C, and ^{15}N chemical shifts in AR were assigned on the basis of three-dimensional (3D) ^{15}N-edited TOCSY (mixing time of 70 ms), HNCACB, CBCA(CO)NH, C-(CCO)NH, HNCO, and HN(CA)CO spectra, and the secondary structure propensity (SSP) scores were calculated from the $^{13}C^{\alpha}$, $^{13}C^{\beta}$, and $^{1}H^{\alpha}$ chemical shifts.[49] The steady-state ^{1}H−^{15}N nuclear Overhauser effect (NOE) was measured using two-dimensional (2D) heteronuclear correlation experiments. Both spectra with and without ^{1}H saturation were acquired with a 2 s relaxation delay followed by a 3 s saturation delay; the saturation power in the experiment without saturation was set to the minimum.

Signals in 2D ^{1}H−^{15}N heteronuclear single-quantum correlation (HSQC) spectra of ^{15}N-labeled AR-N and AR-C were assigned on the basis of the similarity to the HSQC spectrum of AR. To investigate binding of RbAB to the RIZ constructs, unlabeled RbAB was added to samples of ^{15}N-labeled AR, AR-N, or AR-C, the samples were reconcentrated to their initial volume using Amicon Ultra filter units with a 3 kDa molecular mass cutoff (Millipore), and ^{1}H−^{15}N HSQC spectra were acquired.

Isothermal Titration Calorimetry (ITC). Protein samples for ITC were dialyzed extensively against Tris buffer [20 mM

DOI: 10.1021/bi501398w
Biochemistry 2015, 54, 1390−1400

Tris (pH 7.5), 140 mM NaCl, and 2 mM β-mercaptoethanol], and lyophilized peptides were dissolved directly in the buffer. ITC experiments were conducted in a VP-ITC instrument (MicroCal, GE Healthcare) at 25 °C. For direct binding experiments, 8 μL aliquots of RbAB were injected into the calorimeter cell containing a 1.43 mL solution of AR, AR-N, or AR-C, and the heats of binding were recorded. The data were analyzed with the ORIGIN software provided with the ITC instrument.

The affinity of RbAB for AR-N and FITC-RIZ(254−267) was also investigated by a competition-based method,[50] titrating AR-C into RbAB in the presence of a large excess of AR-N or FITC-RIZ(254−267). The association constant for the interaction of RbAB with AR-N or FITC-RIZ(254−267) was then determined from the apparent association constant using eq 21 from ref 50.

Fluorescence Anisotropy. All fluorescence measurements were taken at 20 or 25 °C in PBS (pH 7.5) supplemented with 2.5 mM DTT. In direct binding assays, the total concentration of the FITC-labeled peptides was kept constant and the concentration of RbAB was varied. In competitive binding assays, the total concentrations of FITC-labeled peptides and RbAB were kept constant and the concentration of the competitor (AR-N or AR-C) was varied.

The experiments were performed using time-correlated single-photon counting (TCSPC) as described in ref 51. Steady-state anisotropy values were obtained from the data with the FluoFit Pro version 4.2.1 analysis software package (PicoQuant, Berlin, Germany). The steady-state values were then analyzed as described in ref 52 using eq 6 for the direct binding assays, eq 17 for the competitive binding assays, and eq 40 that describes the relationship between the observed steady-state anisotropy and the fraction of bound FITC-labeled peptide. The ratio of quantum yields for the bound and free fluorophore, Q, was determined from fluorescence intensities of a sample containing 0.65 μM FITC-RIZ(309−319) in the presence or absence of 32.5 μM RbAB. This value of Q was also used for FITC-RIZ(254−267), whose fluorescence intensity in the bound form was difficult to evaluate because of the low affinity for RbAB. The dissociation constants and the fluorescence anisotropies of bound and free FITC peptides were obtained by nonlinear least-squares fitting of the binding curves in MATLAB version 2012a (MathWorks Inc., Natick, MA), using bisquare weights and the trust-region algorithm.

RESULTS

To characterize the AR, we cloned, expressed, and purified the corresponding sequence from human RIZ (residues 197−341). AR eluted from a Superdex 75 size-exclusion column in a volume similar to that of the 60 kDa bovine albumin standard (data not shown), suggesting that it either formed oligomers or adopted an extended conformation in solution. Signals in NMR spectra of AR displayed narrow line widths and limited dispersion typical of unfolded proteins (Figure 3), and the absence of residues with positive heteronuclear ^{1}H−^{15}N NOE indicated that AR is highly flexible (Figure 4). To characterize AR in more detail, we assigned most of the $^{1}H^{N}$, ^{15}N, ^{13}C′, $^{13}C^{\alpha}$, $^{13}C^{\beta}$, and $^{1}H^{\alpha}$ chemical shifts (Figures 2 and 3) and calculated the secondary structure propensity (SSP) scores (Figure 5).[49] For residues in fully formed α-helical or β-strand/extended structures, the SSP scores are expected to be close to +1 or −1, respectively. However, there are virtually no residues in AR that have SSP scores higher than 0.2 or lower than −0.2,

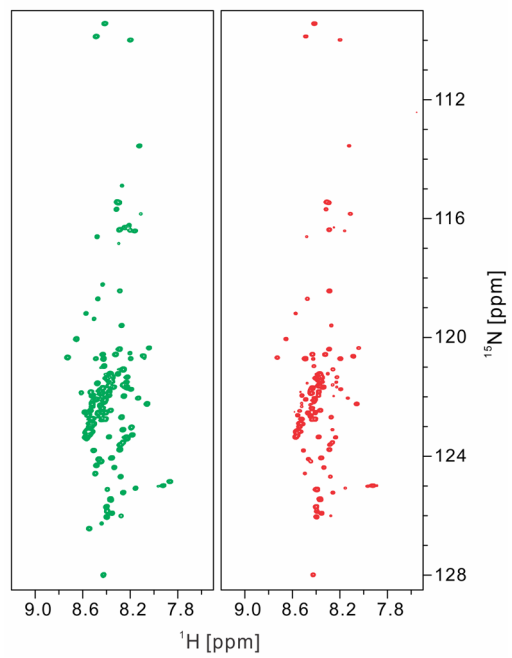

Figure 4. ^{1}H−^{15}N heteronuclear NOE in AR. A reference spectrum without ^{1}H saturation is shown in the left panel, and a ^{1}H−^{15}N NOE spectrum with ^{1}H saturation is shown in the right panel. Positive and negative contour levels are colored green and red, respectively. There are no observable positive signals in the ^{1}H−^{15}N NOE spectrum.

suggesting that AR contains little or no secondary structure. Hence, our data are consistent with AR being intrinsically disordered.

Because AR was reported to bind to the pocket domain of Rb,[21] we next set out to confirm the interaction between the purified components using NMR spectroscopy and to identify the residues in AR that contact the pocket domain. As increasing amounts of unlabeled RbAB were added to ^{15}N-labeled AR, some AR signals gradually diminished and eventually disappeared from 2D ^{1}H−^{15}N HSQC spectra, but no new signals became observable over the range of RbAB concentrations studied (Figures 6A and 7). This behavior is consistent with exchange between the free and bound forms on an intermediate time scale.

Residues 306−322 (KEPEIRCDEKPEDLLEE) were the most affected by RbAB binding (Figure 7). This sequence contains the IRCDE motif that was proposed to mediate the interaction with Rb.[21] Surprisingly, residues 255−267 (RLEAAACEVNDLG) were also affected, but the decrease in their signal intensities was delayed relative to that of residues 306−322 (Figure 7). This suggested that the pocket domain binds preferentially to residues 306−322 and that it interacts with residues 255−267 with a lower affinity. When a large excess of peptide containing the IRCDE motif was added to AR and RbAB, the intensity of all AR signals was restored and the ^{1}H−^{15}N HSQC spectrum became virtually indistinguishable from the spectrum of free AR (Figure 6B). These data indicate that AR binding to RbAB is specific, and that saturating the site on RbAB that binds the IRCDE motif blocks not only the interaction with AR residues 306−322 but also that with residues 255−267.

To obtain more quantitative information about the interaction of AR with the pocket domain, we performed ITC experiments. A single binding event with a dissociation

DOI: 10.1021/bi501398w
Biochemistry 2015, 54, 1390−1400

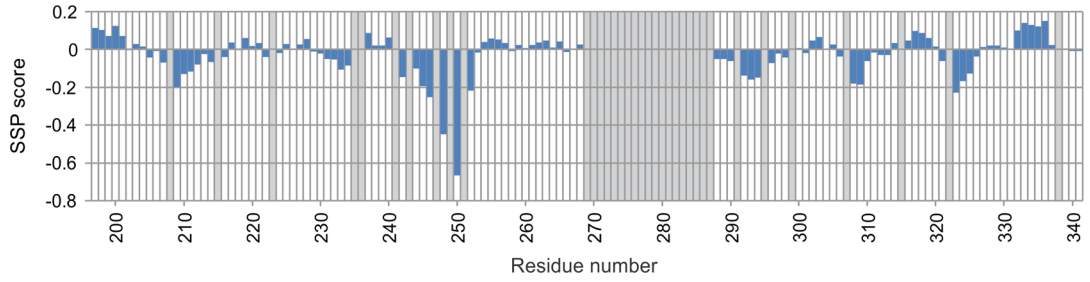

Figure 5. Secondary structure propensity (SSP) of AR. Positive SSP values indicate the expected fractions of α-helical structure at the given positions, and negative values indicate the fractions of β-strand or extended structure. Residues for which no SSP scores were calculated, either because of a lack of assignments (269−287, 291, and 295) or because they precede proline, are colored gray.

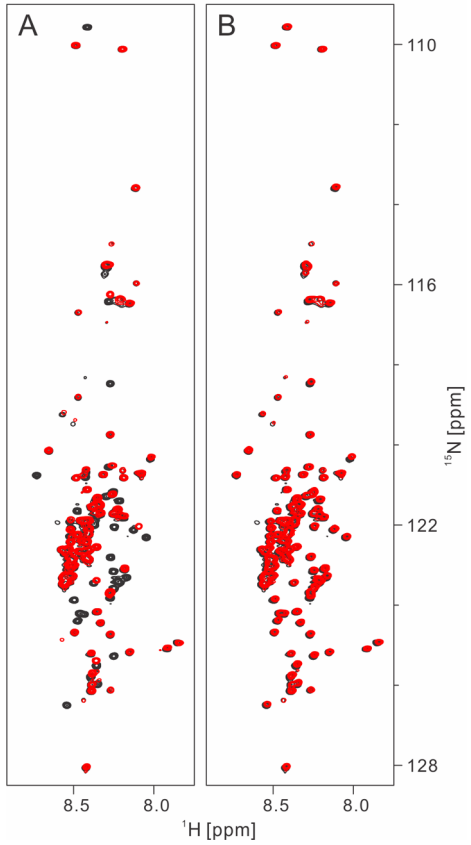

Figure 6. Effect of RbAB on NMR spectra of AR. (A) Superimposed 2D ^{1}H−^{15}N HSQC spectra of 86 μM ^{15}N-labeled AR alone (black) or in the presence of an ∼2-fold molar excess of RbAB (red). (B) Same as panel A, but the sample with 86 μM ^{15}N-labeled AR and an ∼2-fold molar excess of RbAB (red) also contained a 34-fold molar excess of the RIZ(309−319) peptide.

constant (K_d) of 480 nM was observed (Figure 8A and Table 1). However, the additional interaction that was detected by NMR-monitored titration (Figure 7) was not apparent in the ITC data (Figure 8A).

The two sequences whose NMR signals are affected by RbAB, residues 255−267 and 306−322, are located in the N-terminal half and the C-terminal third of AR, respectively, and are separated by a highly degenerate sequence composed mainly of Glu and Asp residues (Figure 7). Hence, to gain more insight into the role of residues 255−267 and 306−322 in Rb binding, we cloned, expressed, and purified two shorter constructs, AR-N and AR-C (Figures 1 and 2). Residues 255−267 were included in AR-N, and residues 306−322 were in the AR-C construct, which allowed us to investigate the two sequences separately.

The 2D ^{1}H−^{15}N HSQC spectra of AR-N and AR-C are shown in Figure 9. For virtually every signal in these spectra, there is a counterpart at the same position in the ^{1}H−^{15}N HSQC spectrum of AR (data not shown). This indicates that the ^{1}H and ^{15}N amide chemical shifts in the shorter AR-N and AR-C constructs are the same as in the longer AR construct, consistent with absence of long-range interactions between residues 197−269 or 297−341 and the rest of AR. Upon addition of RbAB, the intensity of certain peaks in the 2D ^{1}H−^{15}N HSQC spectra of AR-N and AR-C decreased dramatically (Figure 9). Residues 255−267 in AR-N and residues 307−322 in AR-C were the most affected (Figure 10), similar to what we observed in the NMR-monitored titrations of AR with RbAB (Figure 6). Our results demonstrate that RbAB can interact with each site independently.

With AR-N and AR-C in hand, we proceeded to separately measure the affinity of each site for RbAB by ITC. AR-C bound to RbAB with a K_d of 640 nM, but no interaction between AR-N and RbAB was detected (Figure 8B,C and Table 1). Because our NMR data clearly show that AR-N binds RbAB at concentrations comparable to those used in the ITC experiments (Figure 9), we conclude that at 25 °C the enthalpy of binding is too low to be measured and the interaction is primarily entropically driven.

As we were unable to observe the binding of AR-N to RbAB and determine the dissociation constant using direct ITC experiments, we resorted to other methods. We obtained a fluorescein-labeled peptide, FITC-RIZ(254−267), and investigated its interaction with RbAB using fluorescence anisotropy. This peptide included all the residues from AR-N whose NMR signals were affected by RbAB binding (Figures 7 and 10). The interaction of FITC-RIZ(254−267) with RbAB was readily observed by this method (Figure 11A), and fitting of the anisotropy data yielded a K_d of ∼170 μM (Table 2). We also used a competitive binding assay with the FITC-RIZ(254−267) peptide (Figure 11B) and established that AR-N binds to RbAB with comparable affinity (K_d ∼ 90 μM) (Table 2). Fluorescence anisotropy experiments with the FITC-RIZ(309−319) peptide, which contains the IRCDE motif, and competition assays with AR-C (Figure 11C,D) yielded K_d values of ∼360 and ∼110 nM for the interaction of RbAB with the FITC-RIZ(309−319) peptide and AR-C, respectively (Table 2). These values are in the submicromolar range, similar to the dissociation constants that we obtained for the interaction of RbAB with AR-C and AR by ITC (Table 1).

In addition to fluorescence anisotropy, we also used competition-based ITC experiments to measure the affinity of

DOI: 10.1021/bi501398w
Biochemistry 2015, 54, 1390−1400

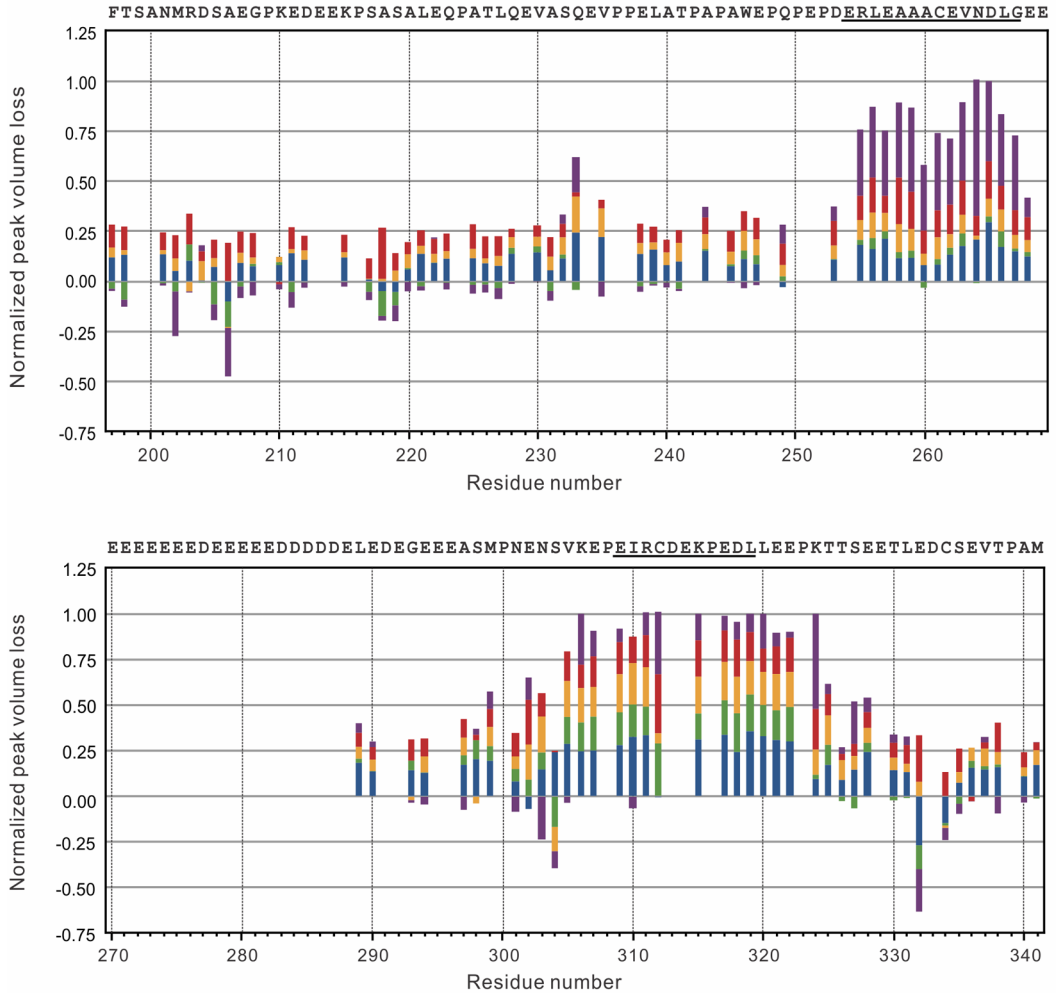

Figure 7. Normalized loss of peak volumes in $^{1}H-^{15}N$ HSQC spectra of AR upon stepwise increases in RbAB concentration. 2D $^{1}H-^{15}N$ HSQC spectra were acquired for 160 μM ^{15}N-labeled AR alone and in the presence of 40, 80, 120, 160, or 200 μM RbAB, and the peak volumes were measured. The loss of peak volume for each increment in RbAB concentration, divided by the peak volume of free AR, is shown as a function of residue number. The blue, green, yellow, red, and purple bars represent the relative peak volume losses when the RbAB concentration was increased from 0 to 40 μM, from 40 to 80 μM, from 80 to 120 μM, from 120 to 160 μM, and from 160 to 200 μM, respectively. When the peaks completely disappear, the stacked up bars reach a value of 1. The AR sequence is displayed on top for reference, and the sequences of the synthetic peptides that were used to further investigate the interaction of RbAB with the two most affected regions are underlined.

AR-N for RbAB. This approach is based on the ability of the IRCDE motif to displace AR-N from RbAB (Figure 6B), and it takes advantage of the fact that at 25 °C little or no heat is released upon binding of AR-N to RbAB while the interaction of AR-C with RbAB is exothermic (Figure 8B,C). The dissociation constants determined by this method, ~70 and 45 μM for the interaction of RbAB with FITC-RIZ(254−267) and AR-N, respectively (Table 3), are comparable to the dissociation constants obtained by fluorescence anisotropy (Table 1).

DISCUSSION

Rb has been reported to interact with many cellular targets.[35] However, it is important to note that most studies do not distinguish between proteins that directly contact Rb and proteins that are only indirectly associated. Hence, a number of interactions between Rb and its reported partners could not be reproduced using purified recombinant components,[53] suggesting that the proteins interact only functionally but not physically, or that an additional bridging molecule or molecules are required to mediate the contact. To further complicate matters, the mere presence of the consensus Rb-binding LXCXE sequence in the reported Rb interaction partners does not necessarily mean that this sequence mediates binding to Rb. For example, an LXCXE sequence in BRG1 apparently does not bind to the purified pocket domain of Rb, and an LXCXE-like sequence from histone deacetylase 1 (HDAC1) interacts with the pocket domain with only modest affinity (K_d ~ 10 μM).[42] It is conceivable that residues other than the consensus Leu, Cys, and Glu modulate the interaction with Rb, and that in some proteins the LXCXE sequence is buried or otherwise masked and hence unavailable for binding to Rb.

Because the AR from RIZ was reported to bind Rb,[21] we set out to investigate the interaction using purified proteins. We show that AR is intrinsically disordered and that it binds RbAB with affinity that is comparable to the affinity of peptides containing the LXCXE motif from viral oncoproteins (K_d ~ 100−200 nM).[26,42] We also demonstrate that the interaction between AR and RbAB is mediated primarily by a short stretch of residues containing the IRCDE motif and that the

DOI: 10.1021/bi501398w
Biochemistry 2015, 54, 1390−1400

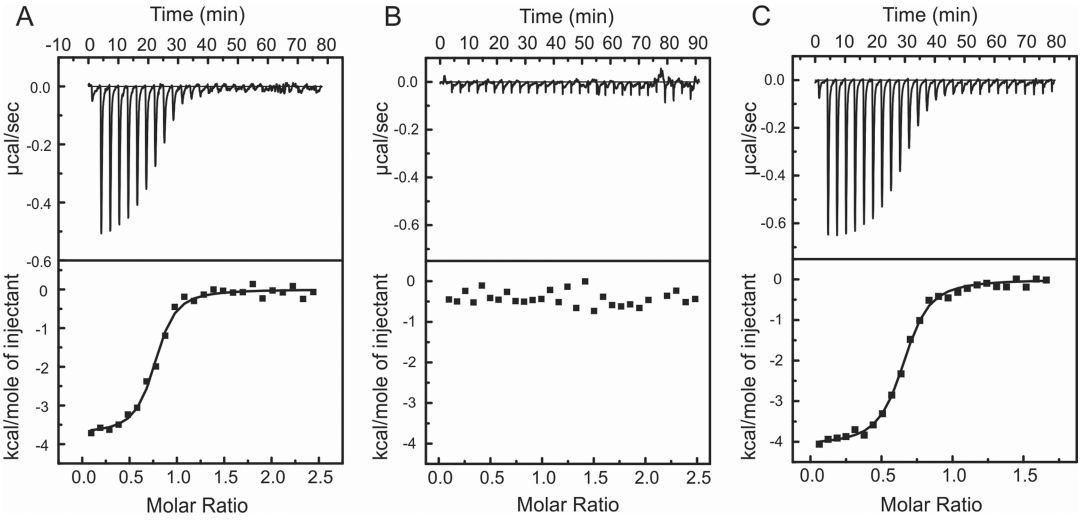

Figure 8. Calorimetric titrations of AR, AR-N, and AR-C with RbAB. Representative ITC traces and binding curves fit to the data using a single-binding site model are shown in the top and bottom panels, respectively. (A) Titration of 28 μM AR with 486 μM RbAB. (B) Titation of 39 μM AR-N with 524 μM RbAB. (C) Titration of 48 μM AR-C with 524 μM RbAB.

Table 1. Dissociation Constants Determined by ITC at 25 °C

interaction	K_d (nM)
RbAB−AR	480 ± 90
RbAB−AR-C	640 ± 70

contribution of other parts of AR to RbAB binding is minimal. The placement of the IRCDE sequence in an intrinsically disordered region might be necessary to ensure optimal accessibility for interaction with Rb. The LXCXE sequences in the viral oncoproteins, in particular in adenoviral E1A,[54] are similarly located in intrinsically disordered regions.

In addition to the IRCDE-containing sequence, RbAB interacts with residues 255−267 (RLEAAACEVNDLG) in AR (Figures 7 and 9). However, binding to these latter residues is at least 2 orders of magnitude weaker and is thus unlikely to be of any physiological relevance. Our competition studies indicate that these residues interact with the LXCXE-binding cleft on RbAB (Figures 6B and 12). Such weak interaction with the LXCXE-binding site that does not involve an LXCXE motif is not without precedent. Similar low-affinity Rb-binding sequence, in addition to a high-affinity LXCXE motif, was also identified in the adenoviral E1A protein.[54] Moreover, a peptide from the E2F2 transcription factor that binds to a different site on Rb with high affinity was found to interact with the LXCXE-binding cleft in one crystal structure.[55] Our data together with these earlier observations suggest that the LXCXE-binding cleft on Rb is prone to weak interactions with a range of sequences that do not conform to the LXCXE consensus motif.

There are currently two structures available that illustrate how LXCXE sequences interact with the pocket domain of Rb. In these structures, Leu, Cys, and Glu in the LXCXE motif and an additional hydrophobic residue (L22, C24, E26, and L28 in the human papilloma virus E7 protein or L103, C105, E107, and M109 in the SV40 large T antigen) mediate most of the contacts with the pocket domain.[26,27] We expect that I310, C312, E314, and P316 in AR contact the pocket domain in an analogous manner. These four residues likely confer most of the Rb binding affinity.

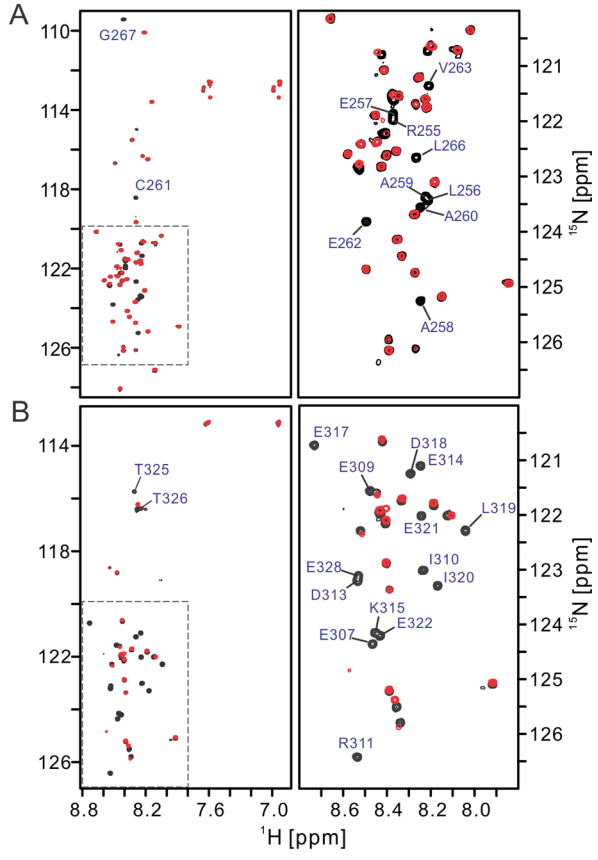

Figure 9. Effect of RbAB on NMR spectra of AR-N and AR-C. (A) Superimposed 2D ^{1}H−^{15}N HSQC spectra of 45 μM ^{15}N-labeled AR-N alone (black) or in the presence of an ∼1.3-fold molar excess of RbAB (red). (B) Superimposed 2D ^{1}H−^{15}N HSQC spectra of 167 μM ^{15}N-labeled AR-C alone (black) or in the presence of an ∼1.4-fold molar excess of RbAB (red). For each construct, the spectral region that is boxed in the left panel is shown expanded on the right, and assignments for the signals that are the most affected by RbAB are indicated.

Our NMR experiments indicate that residues 306−322 in AR (KEPEIRCDEKPEDLLEE) are affected by RbAB binding. This

DOI: 10.1021/bi501398w
Biochemistry 2015, 54, 1390−1400

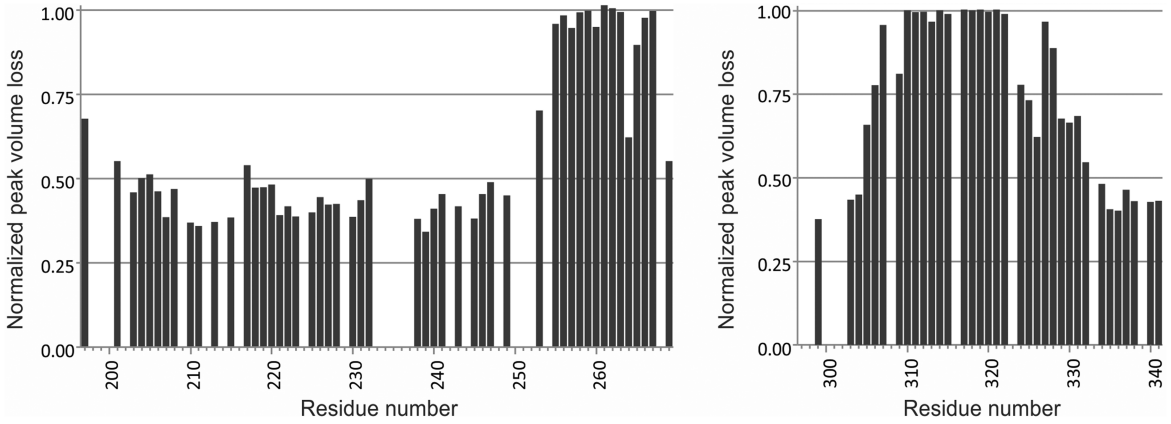

Figure 10. Normalized loss of peak volumes in $^{1}H-^{15}N$ HSQC spectra of AR-N and AR-C upon addition of RbAB. Peak volumes were measured in the spectra of AR-N and AR-C that are shown in Figure 9, and the peak volume loss upon addition of RbAB was divided by the peak volume in the absence of RbAB. The data on the left are for AR-N, and the data on the right are for AR-C.

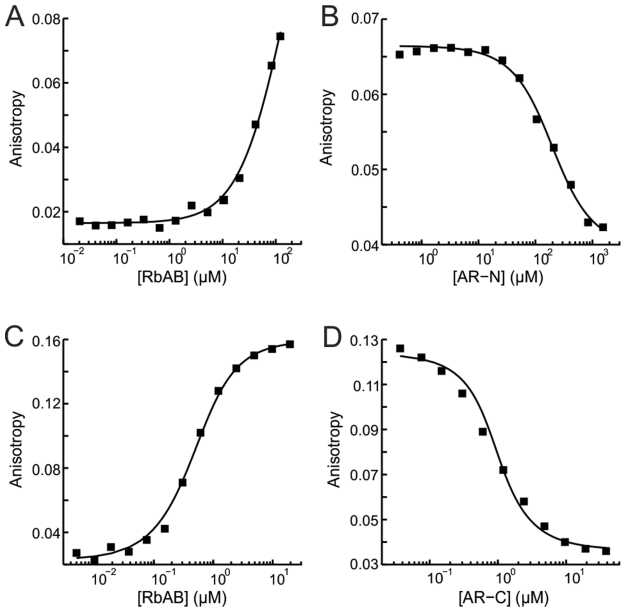

Figure 11. Fluorescence anisotropy binding assays. (A) Direct binding experiment with 0.33 μM FITC-RIZ(254−267) and the concentration of RbAB varied. (B) Competitive binding experiment with 0.33 μM FITC-RIZ(254−267), 91 μM RbAB, and the concentration of AR-N varied. (C) Direct binding experiment with 0.40 μM FITC-RIZ(309−319) and the concentration of RbAb varied. (D) Competitive binding experiment with 0.20 μM FITC-RIZ(309−319), 0.80 μM RbAB, and the concentration of AR-C varied. The binding curves fit to the data are shown as black lines. The experiments with FITC-RIZ(254−267) and FITC-RIZ(309−319) were performed at 25 and 20 °C, respectively.

sequence includes I310, C312, E314, and P316 (bold), and it also contains a number of negatively charged residues [E307, E309, D313, E317, D318, E321, and E322 (underlined)]. These aspartates and glutamates may contribute to RbAB binding by electrostatically interacting with the positively charged lysines (K713, K720, K722, K729, K740, and K765) that flank the LXCXE-binding cleft on Rb. The FITC-RIZ(309−319) peptide that was used for the fluorescence anisotropy experiments is slightly shorter than the sequence implied in Rb binding by NMR spectroscopy. It contains I310, C312, E314, and P316 but lacks several of the acidic residues (E307, E321, and E322). This may explain why FITC-RIZ(309−319) interacts with RbAB with an affinity (K_d ~ 360 nM) slightly lower than that of a longer construct, AR-C (K_d ~ 110 nM) (Table 3).

Table 2. Dissociation Constants Determined from Direct and Competition-Based Fluorescence Anisotropy Experiments

interaction	temp (°C)	K_d[a]
RbAB−FITC-RIZ(309−319)	20	360 nM (270 nM, 460 nM)
RbAB−AR-C	20	110 nM (30 nM, 190 nM)
RbAB−FITC-RIZ(254−267)	25	170 μM (70 μM, 260 μM)
RbAB−AR-N	25	90 μM (50 μM, 120 μM)

[a]The 95% confidence intervals obtained by nonlinear least-squares fitting in MATLAB are shown in parentheses.

Table 3. Dissociation Constants Determined by Competition-Based ITC at 25 °C

interaction	K_d (μM)
RbAB−FITC-RIZ(254−267)	70 ± 10
RbAB−AR-N	45 ± 20

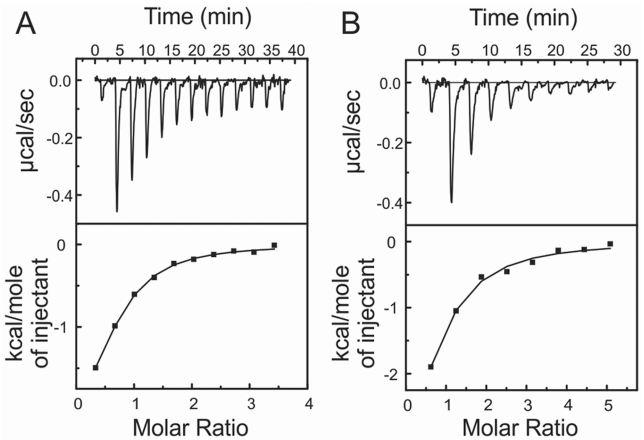

Figure 12. Calorimetric titrations of RbAB with AR-C in the presence of FITC-RIZ(254−267) or AR-N. (A) Titration of 20 μM RbAB with 1154 μM AR-C in the presence of 650 μM FITC-RIZ(254−267). (B) Titration of 9 μM RbAB with 984 μM AR-C in the presence of 459 μM AR-N. Representative ITC traces and binding curves fit to the data are shown in the top and bottom panels, respectively.

DOI: 10.1021/bi501398w
Biochemistry 2015, 54, 1390−1400

It was suggested previously that positively charged amino acids in the XLXCXEXXX sequence significantly weaken the interaction with the pocket domain.[42] There are two positively charged residues present in this region of AR (EI**R**CDE**K**PE), yet the affinity of this sequence for the pocket domain is comparable to or better than the affinities of some LXCXE sequences that contain no lysines or arginines.[42] Hence, while positively charged residues at certain positions may be detrimental to Rb binding, our results show that this is not generally true for all positions and sequence contexts. AR contains a high number of acidic residues in this region, and it is conceivable that some of them form salt bridges with R311 and/or K316 and thus mask the positive charge.

The PR(SET) domain in RIZ1 was reported to catalyze methylation of K9 in histone H3,[56] which suggests that RIZ1 acts as a chromatin-modifying enzyme. It is therefore tempting to speculate that RIZ1 cooperates with Rb to regulate chromatin structure. However, it should be noted that some residues that are highly conserved in canonical SET domains and believed to be important for their histone lysine methyltransferase (HKMT) activity are not conserved in the PR(SET) domain of RIZ1, and the intrinsic enzymatic activity of constructs containing the PR(SET) domain of RIZ1 is very low. Purified recombinant RIZ(1−161), RIZ(1−200), and RIZ(9−359) proteins interact only weakly with *S*-adenosyl-L-methionine and histone peptide substrates, and their HKMT activity cannot be detected by mass spectrometry or Western blotting (ref 57 and unpublished results). Understanding the molecular basis of the reported RIZ1 HKMT activity and the relevance of this activity for the tumor suppressive function of RIZ1 and Rb will thus require further investigation.

AUTHOR INFORMATION

Corresponding Author

*Department of Chemistry and Biochemistry, University of Montana, 32 Campus Dr., Missoula, MT 59812. E-mail: klara.briknarova@umontana.edu. Phone: (406) 243-4408.

Funding

Research reported in this publication was supported by the Research Grant Program at the University of Montana and National Institutes of Health Grant P20GM103546. The Magnetic Resonance and BioSpectroscopy Core Facilities, at which some of the work was performed, also received support from National Institutes of Health Grant P20GM103546. The 600 MHz NMR spectrometer was purchased with funds from National Science Foundation Grant CHE-0321002 and the Murdock Charitable Trust.

Notes

The authors declare no competing financial interest.

ACKNOWLEDGMENTS

We are grateful to Dr. Shi Huang (State Key Laboratory of Medical Genetics, Central South University) for providing the p3RIZRHQB and pCMV-Rb plasmids, Dr. Celestine Thomas and Dr. Stephen R. Sprang (University of Montana) for making their ITC instrument available to us, and Ms. Michelle Terwilliger (University of Montana) for assistance with the fluorescence anisotropy experiments.

ABBREVIATIONS

2D, two-dimensional; 3D, three-dimensional; AR, acidic region; BCA, bicinchoninic acid; DTT, dithiothreitol; EDTA, ethylenediaminetetraacetic acid; FITC, fluorescein isothiocyanate; GST, glutathione transferase; HDAC1, histone deacetylase 1; HKMT, histone lysine methyltransferase; HSQC, heteronuclear single-quantum correlation; ITC, isothermal titration calorimetry; K_d, dissociation constant; NMR, nuclear magnetic resonance; NOE, nuclear Overhauser effect; pABA, *p*-aminobenzamidine; PBS, phosphate-buffered saline; PCR, polymerase chain reaction; Rb, retinoblastoma protein; RIZ, retinoblastoma protein-interacting zinc finger protein; SSP, secondary structure propensity; SV40, simian virus 40; TCSPC, time-correlated single-photon counting; TEV, tobacco etch virus.

REFERENCES

(1) Xie, M., Shao, G., Buyse, I. M., and Huang, S. (1997) Transcriptional repression mediated by the PR domain zinc finger gene RIZ. *J. Biol. Chem. 272*, 26360−26366.

(2) Muraosa, Y., Takahashi, K., Yoshizawa, M., and Shibahara, S. (1996) cDNA cloning of a novel protein containing two zinc-finger domains that may function as a transcription factor for the human heme-oxygenase-1 gene. *Eur. J. Biochem. 235*, 471−479.

(3) Medici, N., Abbondanza, C., Nigro, V., Rossi, V., Piluso, G., Belsito, A., Gallo, L., Roscigno, A., Bontempo, P., Puca, A. A., Molinari, A. M., Moncharmont, B., and Puca, G. A. (1999) Identification of a DNA binding protein cooperating with estrogen receptor as RIZ (retinoblastoma interacting zinc finger protein). *Biochem. Biophys. Res. Commun. 264*, 983−989.

(4) Abbondanza, C., Medici, N., Nigro, V., Rossi, V., Gallo, L., Piluso, G., Belsito, A., Roscigno, A., Bontempo, P., Puca, A. A., Molinari, A. M., Moncharmont, B., and Puca, G. A. (2000) The retinoblastoma-interacting zinc-finger protein RIZ is a downstream effector of estrogen action. *Proc. Natl. Acad. Sci. U.S.A. 97*, 3130−3135.

(5) Carling, T., Kim, K. C., Yang, X. H., Gu, J., Zhang, X. K., and Huang, S. (2004) A histone methyltransferase is required for maximal response to female sex hormones. *Mol. Cell. Biol. 24*, 7032−7042.

(6) Garcia-Bassets, I., Kwon, Y. S., Telese, F., Prefontaine, G. G., Hutt, K. R., Cheng, C. S., Ju, B. G., Ohgi, K. A., Wang, J., Escoubet-Lozach, L., Rose, D. W., Glass, C. K., Fu, X. D., and Rosenfeld, M. G. (2007) Histone methylation-dependent mechanisms impose ligand dependency for gene activation by nuclear receptors. *Cell 128*, 505−518.

(7) Fog, C. K., Galli, G. G., and Lund, A. H. (2012) PRDM proteins: Important players in differentiation and disease. *BioEssays 34*, 50−60.

(8) Hohenauer, T., and Moore, A. W. (2012) The Prdm family: Expanding roles in stem cells and development. *Development 139*, 2267−2282.

(9) Liu, L., Shao, G., Steele-Perkins, G., and Huang, S. (1997) The retinoblastoma interacting zinc finger gene *RIZ* produces a PR domain-lacking product through an internal promoter. *J. Biol. Chem. 272*, 2984−2991.

(10) Steele-Perkins, G., Fang, W., Yang, X. H., Van Gele, M., Carling, T., Gu, J., Buyse, I. M., Fletcher, J. A., Liu, J., Bronson, R., Chadwick, R. B., de la Chapelle, A., Zhang, X. K., Speleman, F., and Huang, S. (2001) Tumor formation and inactivation of RIZ1, an Rb-binding member of a nuclear protein-methyltransferase superfamily. *Genes Dev. 15*, 2250−2262.

(11) He, L., Yu, J. X., Liu, L., Buyse, I. M., Wang, M., Yang, Q., Nakagawara, A., Brodeur, G. M., Shi, Y. E., and Huang, S. (1998) RIZ1, but not the alternative RIZ2 product of the same gene, is underexpressed in breast cancer, and forced RIZ1 expression causes G_2-M cell cycle arrest and/or apoptosis. *Cancer Res. 58*, 4238−4244.

(12) Du, Y., Carling, T., Fang, W., Piao, Z., Sheu, J. C., and Huang, S. (2001) Hypermethylation in human cancers of the RIZ1 tumor suppressor gene, a member of a histone/protein methyltransferase superfamily. *Cancer Res. 61*, 8094−8099.

(13) Jiang, G., Liu, L., Buyse, I. M., Simon, D., and Huang, S. (1999) Decreased RIZ1 expression but not RIZ2 in hepatoma and suppression of hepatoma tumorigenicity by RIZ1. *Int. J. Cancer 83*, 541−546.

DOI: 10.1021/bi501398w
Biochemistry 2015, 54, 1390−1400

(14) Sasaki, O., Meguro, K., Tohmiya, Y., Funato, T., Shibahara, S., and Sasaki, T. (2002) Altered expression of retinoblastoma protein-interacting zinc finger gene, RIZ, in human leukaemia. *Br. J. Haematol. 119*, 940−948.
(15) Oshimo, Y., Oue, N., Mitani, Y., Nakayama, H., Kitadai, Y., Yoshida, K., Chayama, K., and Yasui, W. (2004) Frequent epigenetic inactivation of RIZ1 by promoter hypermethylation in human gastric carcinoma. *Int. J. Cancer 110*, 212−218.
(16) Lal, G., Padmanabha, L., Smith, B. J., Nicholson, R. M., Howe, J. R., O'Dorisio, M. S., and Domann, F. E. J. (2006) RIZ1 is epigenetically inactivated by promoter hypermethylation in thyroid carcinoma. *Cancer 107*, 2752−2759.
(17) Liu, Z. Y., Wang, J. Y., Liu, H. H., Ma, X. M., Wang, C. L., Zhang, X. P., Tao, Y. Q., Lu, Y. C., Liao, J. C., and Hu, G. H. (2013) Retinoblastoma protein-interacting zinc-finger gene 1 (RIZ1) dysregulation in human malignant meningiomas. *Oncogene 32*, 1216−1222.
(18) Lakshmikuttyamma, A., Takahashi, N., Pastural, E., Torlakovic, E., Amin, H. M., Garcia-Manero, G., Voralia, M., Czader, M., DeCoteau, J. F., and Geyer, C. R. (2009) RIZ1 is potential CML tumor suppressor that is down-regulated during disease progression. *J. Hematol. Oncol. 2*, 28.
(19) Chadwick, R. B., Jiang, G. L., Bennington, G. A., Yuan, B., Johnson, C. K., Stevens, M. W., Niemann, T. H., Peltomaki, P., Huang, S., and de la Chapelle, A. (2000) Candidate tumor suppressor RIZ is frequently involved in colorectal carcinogenesis. *Proc. Natl. Acad. Sci. U.S.A. 97*, 2662−2667.
(20) Jiang, G. L., and Huang, S. (2001) Adenovirus expressing RIZ1 in tumor suppressor gene therapy of microsatellite-unstable colorectal cancers. *Cancer Res. 61*, 1796−1798.
(21) Buyse, I. M., Shao, G., and Huang, S. (1995) The retinoblastoma protein binds to RIZ, a zinc-finger protein that shares an epitope with the adenovirus E1A protein. *Proc. Natl. Acad. Sci. U.S.A. 92*, 4467−4471.
(22) Lee, W. H., Bookstein, R., Hong, F., Young, L. J., Shew, J. Y., and Lee, E. Y. (1987) Human retinoblastoma susceptibility gene: Cloning, identification, and sequence. *Science 235*, 1394−1399.
(23) Talluri, S., and Dick, F. A. (2012) Regulation of transcription and chromatin structure by pRB: Here, there and everywhere. *Cell Cycle 11*, 3189−3198.
(24) Dick, F. A., and Rubin, S. M. (2013) Molecular mechanisms underlying RB protein function. *Nat. Rev. Mol. Cell Biol. 14*, 297−306.
(25) Whyte, P., Williamson, N. M., and Harlow, E. (1989) Cellular targets for transformation by the adenovirus E1A proteins. *Cell 56*, 67−75.
(26) Lee, J. O., Russo, A. A., and Pavletich, N. P. (1998) Structure of the retinoblastoma tumour-suppressor pocket domain bound to a peptide from HPV E7. *Nature 391*, 859−865.
(27) Kim, H. Y., Ahn, B. Y., and Cho, Y. (2001) Structural basis for the inactivation of retinoblastoma tumor suppressor by SV40 large T antigen. *EMBO J. 20*, 295−304.
(28) Liu, X., and Marmorstein, R. (2007) Structure of the retinoblastoma protein bound to adenovirus E1A reveals the molecular basis for viral oncoprotein inactivation of a tumor suppressor. *Genes Dev. 21*, 2711−2716.
(29) Xiao, B., Spencer, J., Clements, A., Ali-Khan, N., Mittnacht, S., Broceno, C., Burghammer, M., Perrakis, A., Marmorstein, R., and Gamblin, S. J. (2003) Crystal structure of the retinoblastoma tumor suppressor protein bound to E2F and the molecular basis of its regulation. *Proc. Natl. Acad. Sci. U.S.A. 100*, 2363−2368.
(30) Isaac, C. E., Francis, S. M., Martens, A. L., Julian, L. M., Seifried, L. A., Erdmann, N., Binné, U. K., Harrington, L., Sicinski, P., Bérubé, N. G., Dyson, N. J., and Dick, F. A. (2006) The retinoblastoma protein regulates pericentric heterochromatin. *Mol. Cell. Biol. 26*, 3659−3671.
(31) Talluri, S., Isaac, C. E., Ahmad, M., Henley, S. A., Francis, S. M., Martens, A. L., Bremner, R., and Dick, F. A. (2010) A G_1 checkpoint mediated by the retinoblastoma protein that is dispensable in terminal differentiation but essential for senescence. *Mol. Cell. Biol. 30*, 948−960.
(32) Bourgo, R. J., Thangavel, C., Ertel, A., Bergseid, J., McClendon, A. K., Wilkens, L., Witkiewicz, A. K., Wang, J. Y. J., and Knudsen, E. S. (2011) RB restricts DNA damage-initiated tumorigenesis through an LXCXE-dependent mechanism of transcriptional control. *Mol. Cell 43*, 663−672.
(33) Coschi, C. H., Martens, A. L., Ritchie, K., Francis, S. M., Chakrabarti, S., Berube, N. G., and Dick, F. A. (2010) Mitotic chromosome condensation mediated by the retinoblastoma protein is tumor-suppressive. *Genes Dev. 24*, 1351−1363.
(34) Francis, S. M., Chakrabarti, S., and Dick, F. A. (2011) A context-specific role for retinoblastoma protein-dependent negative growth control in suppressing mammary tumorigenesis. *PLoS One 6*, e16434.
(35) Morris, E. J., and Dyson, N. J. (2001) Retinoblastoma protein partners. *Adv. Cancer Res. 82*, 1−54.
(36) Magnaghi-Jaulin, L., Groisman, R., Naguibneva, I., Robin, P., Lorain, S., LeVillain, J. P., Troalen, F., Trouche, D., and Harel-Bellan, A. (1998) Retinoblastoma protein represses transcription by recruiting a histone deacetylase. *Nature 391*, 601−605.
(37) Brehm, A., Miska, E. A., McCance, D. J., Reid, J. L., Bannister, A. J., and Kouzarides, T. (1998) Retinoblastoma protein recruits histone deacetylase to repress transcription. *Nature 391*, 597−601.
(38) Nielsen, S. J., Schneider, R., Bauer, U. M., Bannister, A. J., Morrison, A., O'Carroll, D., Firestein, R., Cleary, M., Jenuwein, T., Herrera, R. E., and Kouzarides, T. (2001) Rb targets histone H3 methylation and HP1 to promoters. *Nature 412*, 561−565.
(39) Vandel, L., Nicolas, E., Vaute, O., Ferreira, R., Ait-Si-Ali, S., and Trouche, D. (2001) Transcriptional repression by the retinoblastoma protein through the recruitment of a histone methyltransferase. *Mol. Cell. Biol. 21*, 6484−6494.
(40) Dunaief, J. L., Strober, B. E., Guha, S., Khavari, P. A., Ålin, K., Luban, J., Begemann, M., Crabtree, G. R., and Goff, S. P. (1994) The retinoblastoma protein and BRG1 form a complex and cooperate to induce cell cycle arrest. *Cell 79*, 119−130.
(41) Lai, A., Lee, J. M., Yang, W. M., DeCaprio, J. A., Kaelin, W. G. J., Seto, E., and Branton, P. E. (1999) RBP1 recruits both histone deacetylase-dependent and -independent repression activities to retinoblastoma family proteins. *Mol. Cell. Biol. 19*, 6632−6641.
(42) Singh, M., Krajewski, M., Mikolajka, A., and Holak, T. A. (2005) Molecular determinants for the complex formation between the retinoblastoma protein and LXCXE sequences. *J. Biol. Chem. 280*, 37868−37876.
(43) Buyse, I. M., and Huang, S. (1997) In vitro analysis of the E1A-homologous sequences of RIZ. *J. Virol. 71*, 6200−6203.
(44) Kapust, R. B., Tözsér, J., Fox, J. D., Anderson, D. E., Cherry, S., Copeland, T. D., and Waugh, D. S. (2001) Tobacco etch virus protease: Mechanism of autolysis and rational design of stable mutants with wild-type catalytic proficiency. *Protein Eng. 14*, 993−1000.
(45) Pace, C. N., Vajdos, F., Fee, L., Grimsley, G., and Gray, T. (1995) How to measure and predict the molar absorption coefficient of a protein. *Protein Sci. 4*, 2411−2423.
(46) Haughland, R. P. (2005) *The Handbook: A Guide to Fluorescent Probes and Labeling Technologies*, 10th ed., Invitrogen Corp., Carlsbad, CA.
(47) Delaglio, F., Grzesiek, S., Vuister, G. W., Zhu, G., Pfeifer, J., and Bax, A. (1995) NMRPipe: A multidimensional spectral processing system based on UNIX pipes. *J. Biomol. NMR 6*, 277−293.
(48) Vranken, W. F., Boucher, W., Stevens, T. J., Fogh, R. H., Pajon, A., Llinás, M., Ulrich, E. L., Markley, J. L., Ionides, J., and Laue, E. D. (2005) The CCPN data model for NMR spectroscopy: Development of a software pipeline. *Proteins 59*, 687−696.
(49) Marsh, J. A., Singh, V. K., Jia, Z., and Forman-Kay, J. D. (2006) Sensitivity of secondary structure propensities to sequence differences between α- and γ-synuclein: Implications for fibrillation. *Protein Sci. 15*, 2795−2804.
(50) Zhang, Y. L., and Zhang, Z. Y. (1998) Low-affinity binding determined by titration calorimetry using a high-affinity coupling ligand: A thermodynamic study of ligand binding to protein tyrosine phosphatase 1B. *Anal. Biochem. 261*, 139−148.

DOI: 10.1021/bi501398w
Biochemistry 2015, 54, 1390−1400

(51) Minazzo, A. S., Darlington, R. C., and Ross, J. B. A. (2009) Loop dynamics of the extracellular domain of human tissue factor and activation of factor VIIa. *Biophys. J. 96*, 681−692.
(52) Roehrl, M. H. A., Wang, J. Y., and Wagner, G. (2004) A general framework for development and data analysis of competitive high-throughput screens for small-molecule inhibitors of protein-protein interactions by fluorescence polarization. *Biochemistry 43*, 16056−16066.
(53) Smialowski, P., Singh, M., Mikolajka, A., Majumdar, S., Joy, J. K., Nalabothula, N., Krajewski, M., Degenkolbe, R., Bernard, H. U., and Holak, T. A. (2005) NMR and mass spectrometry studies of putative interactions of cell cycle proteins pRb and CDK6 with cell differentiation proteins MyoD and ID-2. *Biochim. Biophys. Acta 1750*, 48−60.
(54) Ferreon, J. C., Martinez-Yamout, M. A., Dyson, H. J., and Wright, P. E. (2009) Structural basis for subversion of cellular control mechanisms by the adenoviral E1A oncoprotein. *Proc. Natl. Acad. Sci. U.S.A. 106*, 13260−13265.
(55) Lee, C., Chang, J. H., Lee, H. S., and Cho, Y. (2002) Structural basis for the recognition of the E2F transactivation domain by the retinoblastoma tumor suppressor. *Genes Dev. 16*, 3199−3212.
(56) Kim, K. C., Geng, L., and Huang, S. (2003) Inactivation of a histone methyltransferase by mutations in human cancers. *Cancer Res. 63*, 7619−7623.
(57) Briknarová, K., Zhou, X., Satterthwait, A., Hoyt, D. W., Ely, K. R., and Huang, S. (2008) Structural studies of the SET domain from RIZ1 tumor suppressor. *Biochem. Biophys. Res. Commun. 366*, 807−813.

DOI: 10.1021/bi501398w
Biochemistry 2015, 54, 1390−1400